Electron Accumulation on Naphthalene Diimide Photosensitized by [Ru(2,2'-Bipyridine)3]2+

SCHOLARONE™
Manuscripts

1
2
3
4
5
6
7
8
9
10
11
12
13
14
15
16
17
18
19
20
21
22
23
24
25
26
27
28
29
30
31
32
33
34
35
36
37
38
39
40
41
42
43
44
45
46
47
48
49
50
51
52
53
54
55
56
57
58
59
60

Electron Accumulation on Naphthalene Diimide Photosensitized by [Ru(2,2'-Bipyridine)$_3$]$^{2+}$

Michael Skaisgirski, Xingwei Guo, and Oliver S. Wenger*

Department of Chemistry, University of Basel, St. Johanns-Ring 19, 4056 Basel, Switzerland

ABSTRACT

In a molecular triad comprised of a central naphthalene diimide (NDI) unit flanked by two [Ru(bpy)$_3$]$^{2+}$ (bpy = 2,2'-bipyridine) sensitizers, NDI^{2-} is formed after irradiation with visible light in de-aerated CH$_3$CN in presence of excess triethylamine. The mechanism for this electron accumulation involves a combination of photoinduced and thermal elementary steps. In a structurally related molecular pentad with two peripheral triarylamine (TAA) electron donors attached covalently to a central [Ru(bpy)$_3$]$^{2+}$-NDI-[Ru(bpy)$_3$]$^{2+}$ core but no sacrificial reagents present, photoexcitation only leads to NDI$^-$ (and TAA$^+$), whereas NDI^{2-} is unattainable due to rapid electron transfer events counteracting charge accumulation. For solar energy conversion, this finding means that fully integrated systems with covalently linked photosensitizers and catalysts are not necessarily superior to multi-component systems, because the fully integrated

systems can suffer from rapid undesired electron transfer events that impede multi-electron reactions on the catalyst.

INTRODUCTION

In order to perform multi-electron redox chemistry using visible light as an energy input, it is desirable to understand the basic principles of the photo-driven accumulation of redox equivalents.[1,2] Many prior studies employed sacrificial reagents to generate solar fuels using various molecular catalysts, but often the focus was mainly on product formation rather than on understanding the key elementary step of charge accumulation.[3-15] Photosensitizers and catalysts are often attached covalently to each other, but in some cases the resulting fully integrated assemblies do not exhibit strongly improved properties compared to multi-component systems in which there are no covalent linkages between individual components or reactants. Against this background, we became interested in performing a direct comparison of light-induced charge accumulation in multi-component and unimolecular systems with particular focus on mechanistic aspects.

Several prior studies concentrated specifically on the phenomenon of light-driven charge accumulation in artificial molecular systems, as highlighted in three recent reviews.[16-18] Many of the studied systems relied on sacrificial reagents,[19-29] but newer systems (as well as a few older ones) exhibit intramolecular charge accumulation in absence of sacrificial substances.[30-35] Nevertheless, compared to the ordinary photoinduced transfer of single electrons, light-induced charge accumulation is still poorly explored, for example because multiple photons are usually

required to drive multiple electron transfers, and because there can be many processes that counteract charge accumulation after primary charge separation.

Scheme 1. Molecular structures of triad **I** and pentad **II**.
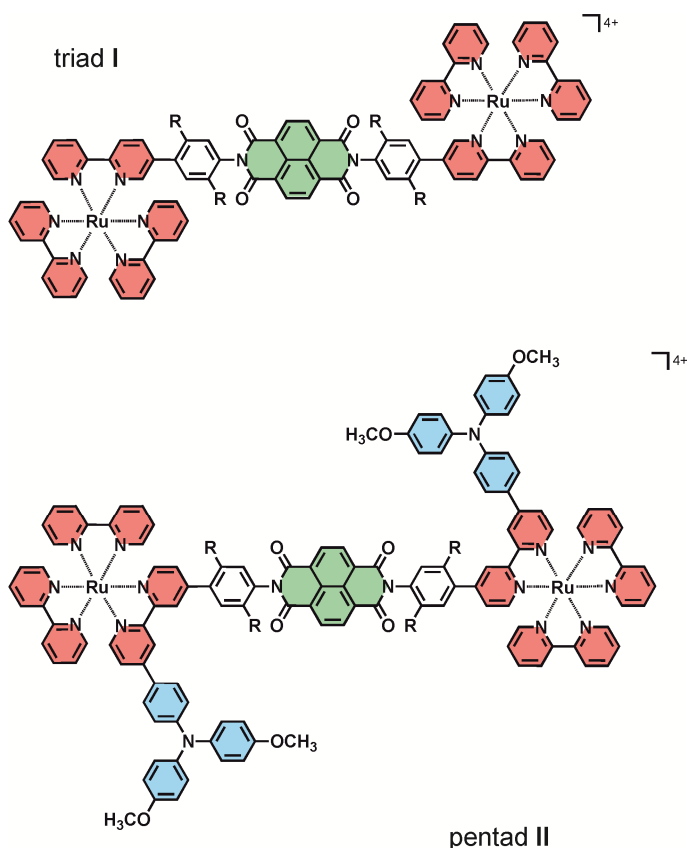
In this work, we explored triad **I** and pentad **II** (Scheme 1) with a view to obtaining doubly reduced naphthalene diimide (NDI^{2-}) after excitation of the covalently attached $[Ru(bpy)_3]^{2+}$ (bpy = 2,2'-bipyridine) photosensitizers with visible light. NDI is well suited for studies with UV-Vis spectroscopy because its neutral, singly, and doubly reduced forms exhibit diagnostic, easily distinguishable signatures.[36] We aimed to explore how charge accumulation on NDI can be achieved with a standard photosensitizer such as $[Ru(bpy)_3]^{2+}$, to understand its mechanisms in

detail, and to obtain insight into the factors limiting its overall efficiency. Through direct comparison of triad **I** (which requires sacrificial electron donors) and pentad **II** (which has covalently attached donors), we aimed to identify advantages and disadvantages of multi-component versus fully integrated (covalently linked) systems for photo-induced charge accumulation, and more generally, for artificial photosynthesis relying on multi-electron chemistry.

RESULTS AND DISCUSSION

Syntheses and characterization data of triad **I** and pentad **II** are reported in the Supporting Information (SI). Both compounds have the $[Ru(bpy)_3]^{2+}$-NDI-$[Ru(bpy)_3]^{2+}$ core motif in common, but with different connectivity between sub-units. This is owed to synthetic challenges faced in the course of attempts to make a pentad which is structurally strictly analogous to triad **I** (i. e., with 5,5'- instead of 4,4'-substituted bpy units). This structural difference is expected to entail significantly stronger electronic communication between sub-units in the pentad because electronic coupling across the 4- and 4'-positions of bpy is usually stronger than across its 5- and 5'-positions.[37,38]

The cyclic voltammograms of **I** and **II** are essentially a superposition of the individual voltammograms of their sub-components (SI, Figure S1 and S2). The first two reductions are NDI-based, whereas $[Ru(bpy)_3]^{2+}$-localized reductions appear at more negative potentials (Table 1).

Table 1. Redox potentials ($E_{1/2}$ in Volts vs. Fc^+/Fc) of the individual components of triad **I** and pentad **II** in CH_3CN at 25 °C. $E_{p,a}$-$E_{p,c}$ (in mV) is the difference in anodic and cathodic peak potentials.

redox couple	triad **I**		pentad **II**	
	$E_{1/2}$ [V]	$E_{p,a}$-$E_{p,c}$ [mV]	$E_{1/2}$ [V]	$E_{p,a}$-$E_{p,c}$ [mV]
TAA^+/TAA	N/A	N/A	0.38	103
NDI/NDI^-	-0.83	82	-0.89	70
NDI^-/NDI^{2-}	-1.33	60	-1.34	65
bpy/bpy^-	-1.53	99	-1.72	112

UV-Vis spectra of **I** and **II** in CH_3CN exhibit the typical MLCT absorptions of the $[Ru(bpy)_3]^{2+}$ chromophores and π-π* transitions on bpy, NDI, and TAA at shorter wavelengths (SI, Figure S3). Selective excitation of the $[Ru(bpy)_3]^{2+}$ chromophore in the visible spectral range is readily possible, but given the direct attachment of *p*-phenylene substituents to one of its bpy ligands, consideration of the ruthenium chromophore as an isolated $[Ru(bpy)_3]^{2+}$ complex is a somewhat crude (but for our purposes nevertheless sufficient) approximation.[39]

Charge accumulation studies were performed on $1.7 \cdot 10^{-5}$ M solutions of **I** in de-aerated CH_3CN containing various concentrations of triethylamine (Et$_3$N) or tetra-*n*-butylammonium 5,6-isopropylidene ascorbate (TBA$^+$ iASc$^-$). Continuous irradiation at 410 nm with a flux of $(3.22\pm0.14) \cdot 10^{16}$ photons / s occurred in a commercial spectrofluorimeter over several minutes (see SI for details). In presence of 0.5 M Et$_3$N, the spectral changes shown in Figure 1a appear in the course of the first 30 s of photo-irradiation.
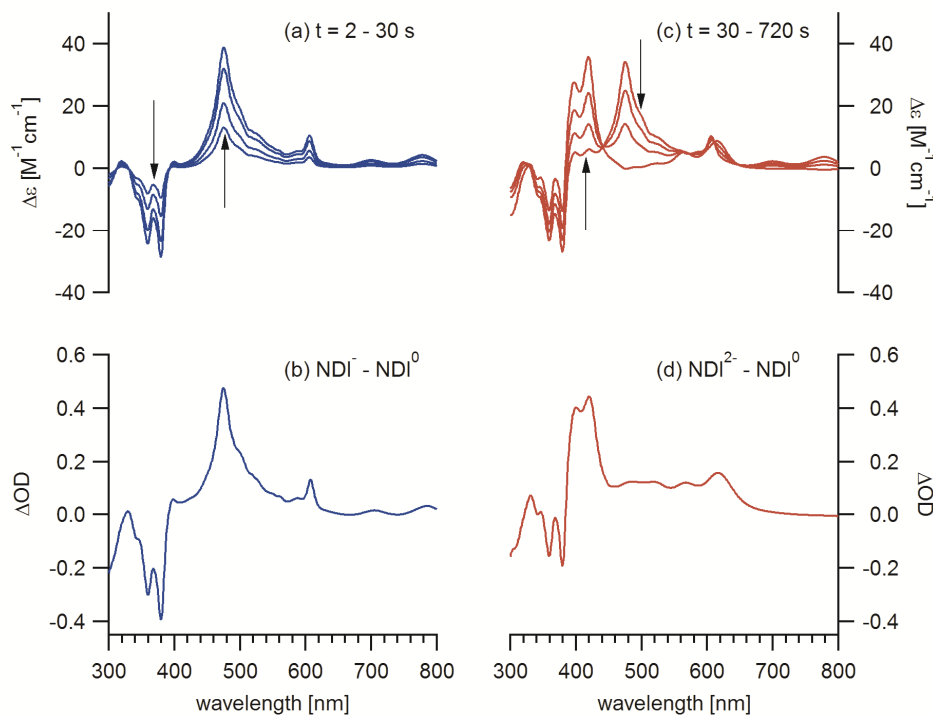
Figure 1. (a) UV-Vis difference spectra measured on a $1.7 \cdot 10^{-5}$ M solution of triad **I** in de-aerated CH_3CN containing 0.5 M Et_3N. Irradiation occurred with a flux of $(3.22 \pm 0.14) \cdot 10^{16}$ photons /s at 410 nm over time intervals ranging from 2 s to 30 s. The spectrum measured at t = 0 s served as a baseline. (b) UV-Vis difference spectrum obtained after chemical reduction of the NDI unit in triad **I** to NDI^-, using benzophenone radical anion in THF as a chemical reductant. The spectrum of the triad prior to reduction served as a baseline. (c) UV-Vis difference spectra of the same solution as in (a) measured after irradiation times between 30 s and 720 s. (d) UV-Vis difference spectrum obtained after reduction of NDI in triad **I** to NDI^{2-} using benzophenone radical anion in THF; the spectrum measured prior to adding the chemical reductant served as a baseline.

Comparison with the UV-Vis difference spectrum obtained from an experiment in which the NDI unit of **I** in dry THF was reduced to NDI^- with benzophenone radical anion (Figure 1b)

shows that the main photochemical reduction product after 30 s is NDI⁻ while [Ru(bpy)₃]²⁺ must

be in its initial (ground) state. Continued irradiation for another 690 s under the same conditions

then induces the spectral changes shown in Figure 1c. The final spectrum is compatible with the

formation of NDI^{2-}, as the comparison with the difference spectrum obtained after chemical

reduction of the NDI unit of **I** to NDI^{2-} in THF (Figure 1d) shows. From the difference spectra, it

becomes evident why 410 nm was chosen for excitation: At this wavelength the changes in

optical density in the course of the conversion of NDI to NDI⁻ and finally NDI^{2-} are

comparatively small, and it remains possible to excite relatively selectively into the [Ru(bpy)₃]²⁺

chromophore. Direct excitation into NDI⁻ or NDI^{2-} could potentially induce energy-wasting

electron transfer events (see below).[17,31,40,41]
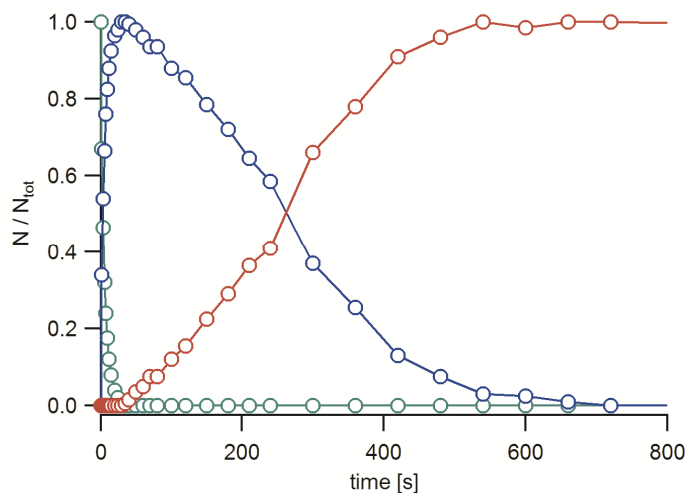
Figure 2. Relative proportions (molar fractions) of NDI (green), NDI⁻ (blue), and NDI^{2-} (red)

present in triad **I** after different irradiation times. The flux used for excitation at 410 nm was

$(3.22\pm0.14)\cdot10^{16}$ photons /s, and the sample contained $3.4\cdot10^{-8}$ mol of triad **I**. This corresponds to

roughly 2 photons per molecule per second. Some of the quantum yields reported in Table 2
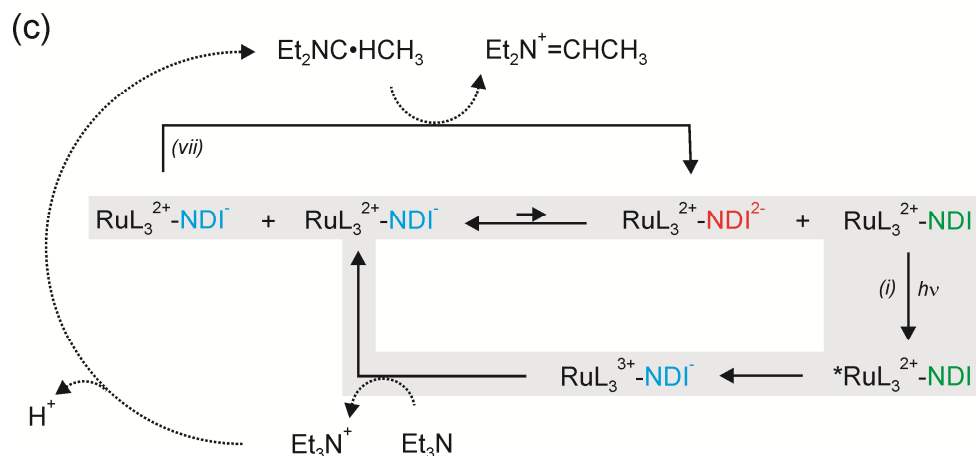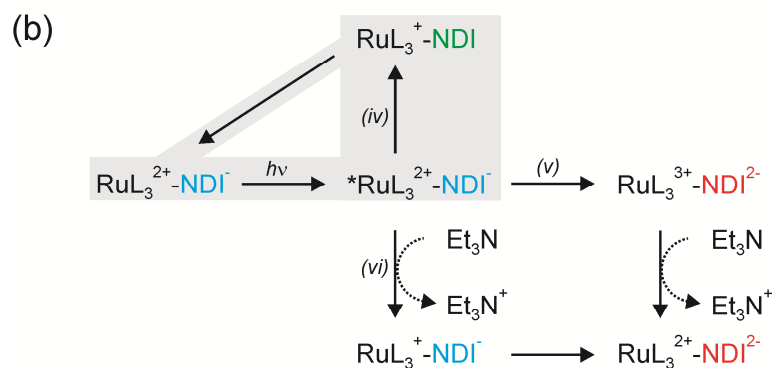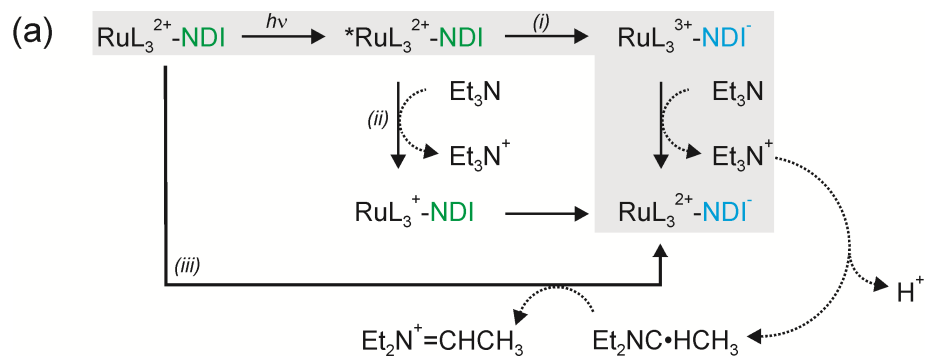
were extracted from this data.

Table 2. Quantum yields for formation of NDI^- and NDI^{2-} when irradiating triad **I** at 410 nm in de-aerated CH_3CN at 25 °C in presence of different concentrations of Et_3N. The experimental uncertainties are ~20%.

$[Et_3N]$ / M	ϕ (NDI $\rightarrow$ NDI$^-$)	ϕ (NDI$^-$ $\rightarrow$ NDI^{2-})
0.10	0.061	0.00026
0.25	0.079	0.00141
0.50	0.107	0.00150

From the difference spectra in Figure 1a and 1c the proportions of NDI^0, NDI^-, and NDI^{2-} at different irradiation times can be determined. The resulting speciation curves (Figure 2) indicate that in presence of 0.5 M Et_3N the population of NDI^- maximizes at ca. 30 s, and after 720 s the formation of NDI^{2-} is essentially complete. When using 0.25 M Et_3N the kinetics are similar, but with 0.1 M Et_3N they are markedly slower (SI, Figures S4 and S5). These irradiation times are obviously dependent on triad concentration and irradiation flux, and consequently it is more meaningful to report quantum yields. In the first few seconds of the conversion of NDI^0 to NDI^-, as well as in the conversion of NDI^- to NDI^{2-}, the growth of the new absorption signals is approximately linear, and we used these (short) time regimes to estimate the quantum yields (ϕ) in Table 2. The key observation is that the conversion of NDI^- to NDI^{2-} has a markedly lower quantum yield than the formation of NDI^- from NDI^0. Not surprisingly, the electron-accumulating step is therefore the more difficult one to accomplish.

Mechanistic insight comes from transient absorption spectroscopy and luminescence quenching experiments. Excitation of triad **I** at 532 nm in de-aerated CH_3CN in absence of Et_3N induces intramolecular electron transfer from photoexcited $[Ru(bpy)_3]^{2+}$ to NDI (SI, Figure S6) with a time constant of 300 ps (SI, Figure S7a). Subsequently, thermal charge recombination, i. e., electron transfer from NDI^- to $[Ru(bpy)_3]^{3+}$, takes place with a time constant of ~20 ns (SI, Figure S7b). For ^{3}MLCT excited-state quenching of $[Ru(bpy)_3]^{2+}$ by Et_3N an upper rate limit of 10^6 M^{-1} s^{-1} has been estimated in prior studies,[42] hence at a concentration of 0.5 M Et_3N, the pseudo first-order rate constant for electron transfer from Et_3N to photoexcited $[Ru(bpy)_3]^{2+}$ is < $5 \cdot 10^5$ s^{-1}. This is more than 6600 times slower than intramolecular photoinduced electron transfer to NDI in triad **I**, and consequently it seems clear that the dominant reaction pathway for the formation of NDI^- in presence of Et_3N involves the sequence of intra- and inter-molecular electron transfer steps shown in Scheme 2a (process (i) rather than process (ii)).

Scheme 2. Reaction pathways leading to electron accumulation in triad **I** in presence of excess Et_3N. (Only one of the two photosensitizers (RuL_3^{2+}) of the triad is indicated for brevity). Gray shaded areas mark the most important pathways. (a) Sequence of reaction steps leading to the formation of NDI^-. (b) Unproductive electron transfer events leading to light absorption but no net photochemistry. (c) Displacement of the (unfavorable) disproportionation equilibrium through continuous removal of NDI^0 and further formation of NDI^{2-} through a thermal reaction with a carbon-centered radical resulting from the decomposition of oxidized Et_3N.

(a)

RuL_3^{2+}-NDI $\xrightarrow{h\nu}$ *RuL_3^{2+}-NDI $\xrightarrow{(i)}$ RuL_3^{3+}-NDI$^-$

(ii) Et$_3$N → Et$_3$N$^+$

Et$_3$N → Et$_3$N$^+$

RuL_3^+-NDI $\longrightarrow$ RuL_3^{2+}-NDI$^-$

(iii)

Et_2N^+=CHCH$_3$ $Et_2NC\bullet HCH_3$ H$^+$

(b)

RuL_3^+-NDI

(iv)

RuL_3^{2+}-NDI$^-$ $\xrightarrow{h\nu}$ *RuL_3^{2+}-NDI$^-$ $\xrightarrow{(v)}$ RuL_3^{3+}-NDI^{2-}

(vi) Et$_3$N → Et$_3$N$^+$

Et$_3$N → Et$_3$N$^+$

RuL_3^+-NDI$^-$ $\longrightarrow$ RuL_3^{2+}-NDI^{2-}

(c)

$Et_2NC\bullet HCH_3$ Et_2N^+=CHCH$_3$

(vii)

RuL_3^{2+}-NDI$^-$ + RuL_3^{2+}-NDI$^-$ $\rightleftharpoons$ RuL_3^{2+}-NDI^{2-} + RuL_3^{2+}-NDI

(i) $h\nu$

RuL_3^{3+}-NDI$^-$ $\longleftarrow$ *RuL_3^{2+}-NDI

H$^+$ Et$_3$N$^+$ Et$_3$N

Following the intramolecular step leading to $[Ru(bpy)_3]^{3+}$ and NDI$^-$, regeneration of $[Ru(bpy)_3]^{2+}$ by Et$_3$N is in competition with intramolecular thermal charge recombination. For the reaction between $[Ru(bpy)_3]^{3+}$ and triethanolamine a rate constant of $1.67\cdot10^7$ M^{-1} s^{-1} has

been reported.[43] Assuming that the reaction with Et_3N is similarly rapid, one expects a pseudo first-order rate constant of $\sim 8 \cdot 10^6$ s^{-1} at an Et_3N concentration of 0.5 M. Since the rate constant for intramolecular charge recombination between $[Ru(bpy)_3]^{3+}$ and NDI^- is $\sim 5 \cdot 10^7$ s^{-1} (time constant of ~ 20 ns, see above), the bimolecular reaction between $[Ru(bpy)_3]^{3+}$ and Et_3N is comparatively slow. This explains why the quantum yields for the formation of NDI^- under the steady-state irradiation conditions are limited to values in the range of $0.061 - 0.107$ (Table 2).

The mechanism leading from NDI^- to NDI^{2-} is more difficult to identify. Spontaneous thermal disproportionation of NDI^- to NDI^{2-} and NDI^0 is not possible, because it is exergonic by 0.4 eV based on the redox potentials for triad **I** (Table 1). When a de-aerated solution of triad **I** in which NDI^- has been formed photochemically with Et_3N is left standing in the dark, NDI^{2-} is not formed (SI, Figure S8a), indicating that further light input is required for the electron-accumulating step. Reductive quenching of ^{3}MLCT-excited $[Ru(bpy)_3]^{2+}$ by Et_3N (process (vi) in Scheme 2b) is slow ($< 5 \cdot 10^5$ s^{-1} at 0.5 M, see above), and intramolecular electron transfer to NDI^- (process (v) in Scheme 2b) is energetically uphill by 0.14 eV based on the potentials in Table 1. Moreover, intramolecular reductive ^{3}MLCT quenching by NDI^- (process (iv) in Scheme 2b) is exergonic by 1.4 eV. Given its high driving-force, this undesired charge shift event is likely to represent the dominant reaction channel after absorption of a photon by triads in which NDI^- is present. This process is expected to be followed by intramolecular thermal charge shift from $[Ru(bpy)_3]^+$ to NDI^0, and the net result is the initial $[Ru(bpy)_3]^{2+}$ / NDI^- couple, but a photon has been consumed (grey shaded area in Scheme 2b). In view of all these pitfalls, the very low quantum yields for the electron-accumulating step (Table 2) become understandable.

After oxidation, Et_3N is known to deprotonate to form the highly reactive $Et_2NC\cdot=CH_3$ radical which is able to reduce $[Ru(bpy)_3]^{2+}$ to $[Ru(bpy)_3]^+$ in the ground state, i. e., in a dark reaction.[44-

[47] However, as noted above, the formation of NDI^{2-} from NDI^- does not proceed in absence of light (SI, Figure S8a), and it seems likely that the $Et_2NC\cdot=CH_3$ radicals react rapidly after they are formed. Presumably, they contribute to the formation of NDI^- already in the course of initial photo-irradiation (Figure 1a), as illustrated in Scheme 2a (process (iii)).

As noted above, spontaneous disproportionation of NDI^- can be excluded on thermodynamic grounds, but this disproportionation equilibrium can be shifted to the product side by constant removal of NDI^0 (Scheme 2c). When the solution contains largely NDI^- (i. e., after 30 s in Figure 1a), a residual concentration of $\sim 10^{-8}$ M^{-1} of NDI^0 is expected in a solution containing an initial triad concentration of $1.7 \cdot 10^{-5}$ M (based on a disproportionation constant of $1.7 \cdot 10^{-7}$ obtained from the redox potentials in Table 1). Prolonged irradiation will eventually bring even this small residual amount of NDI^0 to reaction with Et_3N to afford NDI^-, and with NDI^0 being continuously consumed, more and more NDI^{2-} is formed (grey shaded area in Scheme 2c), also by the reaction of newly produced $Et_2NC\cdot=CH_3$ radicals (process (vii) in Scheme 2c).[44-47] It seems plausible that this thermal overall process (which, however, clearly relies on further light input) is in fact the main electron-accumulating step, particularly in view of the fact that excitation of $[Ru(bpy)_3]^{2+}$ in triads containing NDI^- predominantly induces an unproductive sequence of photoinduced and thermal (intramolecular) charge shift reactions (grey shaded area in Scheme 2b).

With ascorbate as an electron source instead of Et_3N, electron accumulation on NDI is not possible. For solubility reasons, we used tetra-*n*-butylammonium 5,6-isopropylidene ascorbate as a donor and de-aerated methanol for steady-state photoirradiation of triad **I** at 410 nm,[48] but in this experiment not even NDI^- is formed in substantial amounts (SI, Figure S8b). Transient absorption studies demonstrate why: Once NDI^- is formed (SI, Figures S9 and S10), it recombines with ascorbate oxidation products on a timescale of ~ 10 ms (SI, Figure S11). In view

of the fact that ascorbate acts as a nonsacrificial quencher for ^{3}MLCT-excited [Ru(2,2'-bipyrazine)$_3$]$^{2+}$,[49] this finding is not too surprising.

In a separate experiment, we photo-irradiated a three-component mixture containing $1.7 \cdot 10^{-5}$ M of an NDI reference molecule, 2 equivalents of [Ru(bpy)$_3$]$^{2+}$, and 0.5 M Et$_3$N in de-aerated CH$_3$CN but were unable to observe charge accumulation on NDI in this case, possibly due to low cage escape yields (see Supporting Information for details). The quantum yield for formation of NDI$^-$ in this case was 0.070.
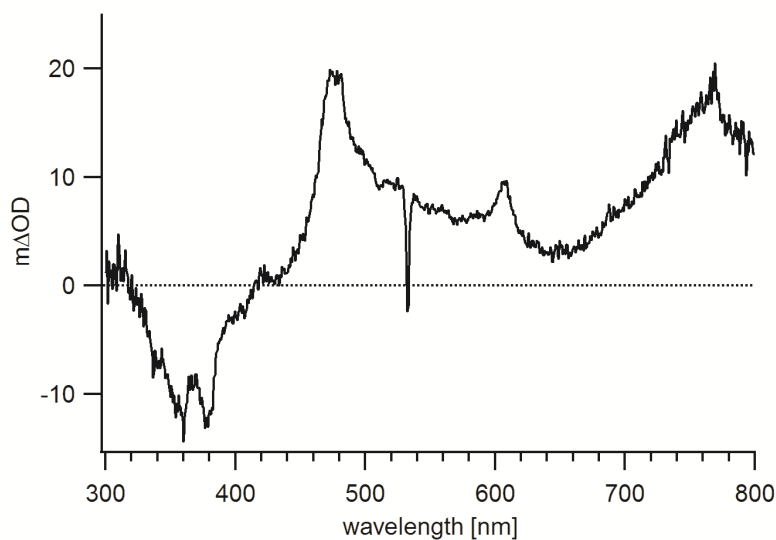
Figure 3. Transient absorption spectrum recorded from a $1.5 \cdot 10^{-5}$ M solution of pentad **II** in de-aerated CH$_3$CN. The sample was excited at 532 nm with laser pulses of ~10 ns duration, and detection occurred by time-integration over 200 ns immediately after excitation. The spike at 532 nm is due to laser stray light.

Pentad **II** has covalently attached TAA donors, and we hoped to achieve entirely intramolecular photoinduced electron accumulation in this case, similar to what we recently

observed in a structurally related system with anthraquinone as a two-electron acceptor.[35]

Excitation of a $1.5 \cdot 10^{-5}$ M solution of pentad **II** at 532 nm with laser pulses of ~10 ns duration

leads to the transient absorption spectrum in Figure 3. The transient absorption bands at 477 and

606 nm signal the formation of NDI$^-$ (SI, Figure S12, Figure 1b) while the bleaches at 355 and

380 nm mark the disappearance of NDI^0 (SI, Figure S3).[36] The band at 765 nm is diagnostic for

TAA$^+$ (SI, Figure S13).[50-52]
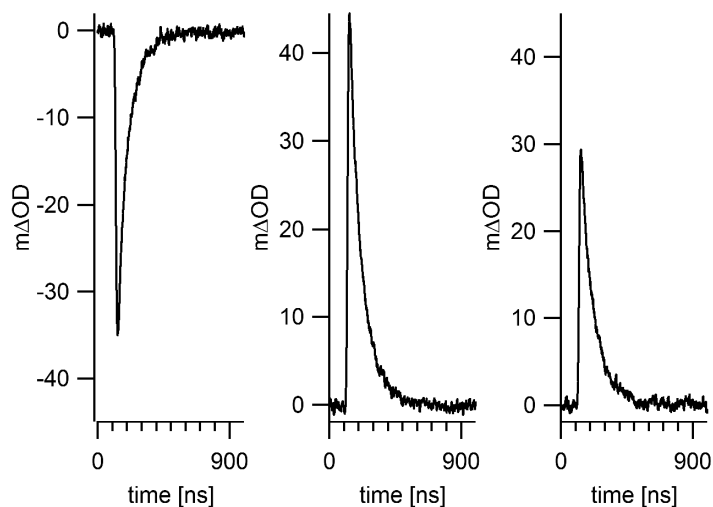
Figure 4. Temporal evolution of the transient absorption signals at (a) 360 nm, (b) 480 nm, and

(c) 770 nm in the spectrum from Figure 3.

The transient absorption signals at 480 and 770 nm form with an instrumentally limited time

constant of 30 ps (SI, Figure S14). They decay in single exponential manner with the same time

constant as the bleach at 360 nm recovers (Figure 4), indicating that (intramolecular) thermal

charge recombination between NDI$^-$ and TAA$^+$ occurs with a time constant of 120 ns in de-

aerated CH$_3$CN at 25 °C. Based on the chemical reduction data in Figure 1d and based on prior

studies,[36] one would expect NDI^{2-} to exhibit characteristic absorption bands at 400, 420, and 615

nm, and we searched carefully for such bands up to very high excitation pulse energies (~30 mJ).

Due to the two-photon nature of the electron accumulation process,[35] the quantity of NDI^{2-}

potentially produced is expected to be very low. For example, in a scenario in which 10% of all

pentads are promoted to the NDI^- / TAA^+ charge-separated state, only ~1% can be expected to be

further promoted to a state in which NDI^{2-} is flanked by 2 TAA^+ units.[31] We were unable to

detect any signals attributable to NDI^{2-}, even when using a sequence of two excitation pulses

(first pulse at 532 nm, 30 mJ; second pulse at 430 nm with a time delay of 50 ns, 21 mJ) in a so-

called two-color pump-pump probe experiment (SI, Figure S15). The second excitation pulse at

430 nm seemed advantageous over excitation with two photons at 532 nm within a single pulse,

because at 430 nm secondary excitation occurs predominantly into the MLCT absorption band of

$[Ru(bpy)_3]^{2+}$, whereas at 532 nm $[Ru(bpy)_3]^{2+}$ only absorbs weakly and there is also some NDI^-

absorption. (Excitation of NDI^- could potentially trigger energy-wasting charge recombination

reactions, but we estimate that under the conditions used in our experiment the absorbance of

photogenerated NDI^- at 532 nm is about 36 times weaker than that of $[Ru(bpy)_3]^{2+}$, hence direct

excitation of NDI^- is expected to be a minor deactivation pathway).

Even successful secondary excitation of $[Ru(bpy)_3]^{2+}$ can trigger unwanted electron transfer

reactions, in particular either reductive excited-state quenching by NDI^- or oxidative quenching

by TAA^+. Both of these processes have significantly higher driving-force than the desired charge

accumulation step leading to NDI^{2-} and 2 TAA^+ units. These types of energy-wasting

photoinduced charge recombination processes seem to be generally the most difficult ones to

avoid when aiming at photoinduced charge accumulation,[31,40,41] and in this regard, multi-

component systems are advantageous compared to fully integrated, covalently linked systems.

This is not only because of the large excess of sacrificial reagents in multi-component systems, but also because the primary oxidation and reduction products can diffuse away from each other, and when absorption of a second photon then takes place, the photoinduced charge recombination events discussed above are far less probable. Furthermore, in multi-component systems the primary charge-separated state (here comprised of NDI⁻ and oxidized Et_3N in the case of **I**) is usually much longer-lived than in covalently connected systems (120 ns for NDI⁻ and TAA^+ in pentad **II**), giving access to the disproportionation chemistry discussed above (Scheme 2c).

Attempts to favor the formation of NDI^{2-} by metal-ion coupled electron transfer (MCET) through addition of the strong Lewis acid Sc^{3+} (50 mM $Sc(OTf)_3$) were unsuccessful.[26,53,54]
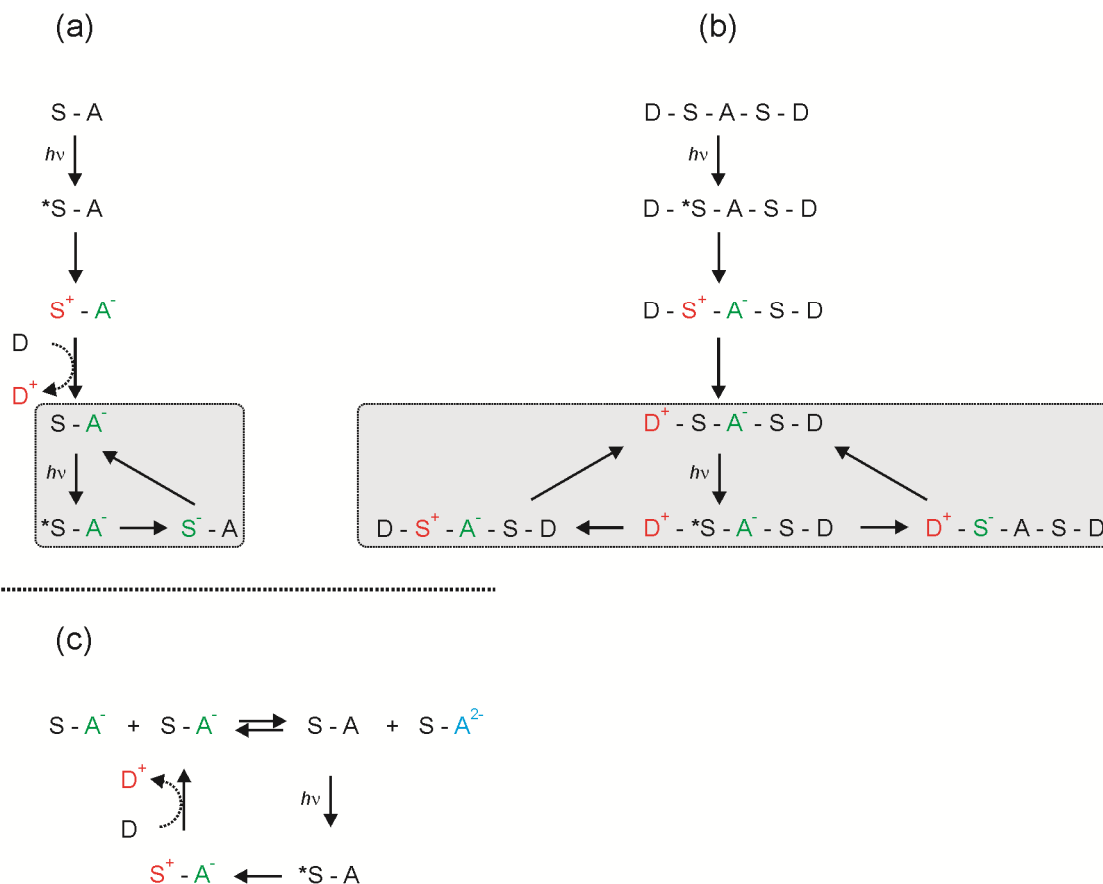
Finally, we note that the ^{3}MLCT excited-state of pentad **II** can in principle be quenched by energy transfer to TAA^+ or NDI⁻. Both radical species have absorptions at wavelengths below 600 nm (Figure 1b, SI, Figures S12 and S13), indicating that they both have excited states which are energetically below the lowest ^{3}MLCT state of $[Ru(bpy)_3]^{2+}$. The NDI⁻ and TAA^+ are doublet species, and it remains to be explored how spin selection rules affect the efficiency of energy transfer in such a case.[55]

SUMMARY AND CONCLUSIONS

Triad **I** is symmetrical with two photosensitizer units for ease of synthesis, but in principle it is functionally analogous to simple sensitizer-acceptor (S-A) dyads. Photoreduction of the NDI unit by one electron in triad **I** is readily possible by the sequence of intra- and intermolecular electron transfer events outlined in Scheme 3a, leading ultimately to the S-A⁻ form. Further excitation of

1
2
3
4
5
6
7
8
9
10
11
12
13
14
15
16
17
18
19
20
21
22
23
24
25
26
27
28
29
30
31
32
33
34
35
36
37
38
39
40
41
42
43
44
45
46
47
48
49
50
51
52
53
54
55
56
57
58
59
60

the latter principally induces reductive excited-state quenching of the sensitizer by A$^-$ because the latter is a strong donor, and the excited sensitizer is a potent acceptor. The resulting S$^-$-A form subsequently reverts spontaneously to the S-A$^-$ form via intramolecular thermal reverse electron transfer (grey shaded area in Scheme 3a). This unproductive (but energy-consuming) sequence of reactions is generally problematic in charge accumulation processes,[17,31,40,41,56] unless A$^-$ is rendered less reducing, for example through protonation in an overall proton-coupled electron transfer (PCET) reaction.[57-59]

Scheme 3. Reaction pathways relevant for electron accumulation in (a) sensitizer-acceptor dyads, and (b) in donor-sensitizer-acceptor-sensitizer-donor pentads. The grey shaded areas mark unproductive yet important electron transfer sequences competing with the electron-accumulating step. (c) Shift of a disproportionation equilibrium through constant removal of the starting material via continuous photoexcitation as a key pathway to charge accumulation.

(a)

S - A

$h\nu \downarrow$

*S - A

$\downarrow$

S^+ - A^-

D

D^+

S - A^-

$h\nu \downarrow$

*S - A^- ⟶ S^- - A

(b)

D - S - A - S - D

$h\nu \downarrow$

D - *S - A - S - D

$\downarrow$

D - S^+ - A^- - S - D

$\downarrow$

D^+ - S - A^- - S - D

$h\nu \downarrow$

D - S^+ - A^- - S - D ⟵ D^+ - *S - A^- - S - D ⟶ D^+ - S^- - A - S - D

(c)

S - A^- + S - A^- ⇌ S - A + S - A^{2-}

D^+

D

$h\nu \downarrow$

S^+ - A^- ⟵ *S - A

In triad **I**, formation of the S-A^{2-} form is only possible thanks to the displacement of the (unfavorable) disproportionation equilibrium in Scheme 3c. Importantly, this thermal reaction requires further light input for continuous removal of the S-A starting material and the concomitant formation of the charge-accumulated S-A^{2-} species. This reaction pathway is only viable with sacrificial donors such as Et$_3$N, but not with reversible donors such as ascorbate. In cases in which the disproportionation of A$^-$ to A and A^{2-} is thermodynamically favored, no further light input is evidently necessary. This should be the case for example in various benzoquinone derivatives.[60,61]

In donor-sensitizer-acceptor-sensitizer-donor pentad **II**, the primary charge-separated state (D$^+$-S-A$^-$-S-A) has a comparatively short lifetime (120 ns), and this makes bimolecular

disproportionation ineffective. Further excitation of the primary charge-separated species predominantly induces the unproductive electron transfer events shown in the grey shaded area of Scheme 3b: The excited state of the sensitizer (*S) is quenched either reductively by A^- or oxidatively by D^+. Again, PCET would be helpful to make A^- less reducing through protonation (see above), and to make D^+ less oxidizing through deprotonation. Phenols would be an interesting choice as one-electron donors, because they usually undergo deprotonation in the course of oxidation.[62-69]

Our direct comparison of a multi-component system (triad **I** with sacrificial donors) and a fully integrated compound (pentad **II** with covalently attached reversible donors) illustrates possible reaction pathways leading to electron accumulation and counteracting processes in both types of approaches. Our study demonstrates that for applications aiming at multi-electron (photo-)redox reactions, the covalent linkage of photosensitizers and catalytic reaction centers introduces significant challenges with regard to avoiding unproductive (but energy-consuming) electron transfer reactions upon sequential absorption of two (or more) photons. These unproductive electron transfers could presumably be decelerated significantly with suitable PCET photochemistry,[70-74] leading ultimately to the accumulation of redox equivalents rather than the accumulation of charge, similar to what is observed in the oxygen-evolving complex of photosystem II.[75,76]

ASSOCIATED CONTENT

Supporting Information. Synthesis protocols, product characterization data, electrochemical, and optical spectroscopic data. This material is available free of charge via the Internet at http://pubs.acs.org.

1
2
3
4
5
6
7
8
9
10
11
12
13
14
15
16
17
18
19
20
21
22
23
24
25
26
27
28
29
30
31
32
33
34
35
36
37
38
39
40
41
42
43
44
45
46
47
48
49
50
51
52
53
54
55
56
57
58
59
60

AUTHOR INFORMATION

Corresponding Author

* oliver.wenger@unibas.ch

Author Contributions

The manuscript was written through contributions of all authors. All authors have given approval

to the final version of the manuscript.

REFERENCES

(1)   Meyer, T. J. Chemical Approaches to Artificial Photosynthesis. *Acc. Chem. Res.*
1989, *22*, 163-170.

(2)   Gray, H. B.; Maverick, A. W. Solar Chemistry of Metal Complexes. *Science*
1981, *214*, 1201-1205.

(3)   Artero, V.; Chavarot-Kerlidou, M.; Fontecave, M. Splitting Water with Cobalt. *Angew. Chem. Int. Ed.* **2011**, *50*, 7238-7266.

(4)   Du, P. W.; Eisenberg, R. Catalysts Made of Earth-Abundant Elements (Co, Ni, Fe) for Water Splitting: Recent Progress and Future Challenges. *Energy Environ. Sci.* **2012**, *5*, 6012-6021.

(5)   Dempsey, J. L.; Brunschwig, B. S.; Winkler, J. R.; Gray, H. B. Hydrogen Evolution Catalyzed by Cobaloximes. *Acc. Chem. Res.* **2009**, *42*, 1995-2004.

(6)   Boston, D. J.; Xu, C. D.; Armstrong, D. W.; MacDonnell, F. M. Photochemical Reduction of Carbon Dioxide to Methanol and Formate in a Homogeneous System with Pyridinium Catalysts. *J. Am. Chem. Soc.* **2013**, *135*, 16252-16255.

(7)   Kobayashi, M.; Masaoka, S.; Sakai, K. Photoinduced Hydrogen Evolution from Water by a Simple Platinum(II) Terpyridine Derivative: A Z-Scheme Photosynthesis. *Angew. Chem. Int. Ed.* **2012**, *51*, 7431-7434.

(8)   Goy, R.; Bertini, L.; Görls, H.; De Gioia, L.; Talarmin, J.; Zampella, G.; Schollhammer, P.; Weigand, W. Silicon-Heteroaromatic FeFe Hydrogenase Model Complexes: Insight into Protonation, Electrochemical Properties, and Molecular Structures. *Chem. Eur. J.* **2015**, *21*, 5061-5073.

(9)   Petermann, L.; Staehle, R.; Pfeifer, M.; Reichardt, C.; Sorsche, D.; Wächtler, M.; Popp, J.; Dietzek, B.; Rau, S. Oxygen-Dependent Photocatalytic Water Reduction with a Ruthenium(imidazolium) Chromophore and a Cobaloxime Catalyst. *Chem. Eur. J.* **2016**, *22*, 8240-8253.

(10)   Herrero, C.; Lassalle-Kaiser, B.; Leibl, W.; Rutherford, A. W.; Aukauloo, A. Artificial Systems Related to Light Driven Electron Transfer Processes in PSII. *Coord. Chem. Rev.* **2008**, *252*, 456-468.

(11)   Windle, C. D.; Perutz, R. N. Advances in Molecular Photocatalytic and Electrocatalytic CO_2 Reduction. *Coord. Chem. Rev.* **2012**, *256*, 2562-2570.

(12)   Luo, S. P.; Mejia, E.; Friedrich, A.; Pazidis, A.; Junge, H.; Surkus, A. E.; Jackstell, R.; Denurra, S.; Gladiali, S.; Lochbrunner, S.; Beller, M. Photocatalytic Water Reduction with Copper-Based Photosensitizers: A Noble-Metal-Free System. *Angew. Chem. Int. Ed.* **2013**, *52*, 419-423.

(13)   Pan, Q.; Freitag, L.; Kowacs, T.; Falgenhauer, J. C.; Korterik, J. P.; Schlettwein, D.; Browne, W. R.; Pryce, M. T.; Rau, S.; Gonzalez, L.; Vos, J. G.; Huijser, A. Peripheral Ligands as Electron Storage Reservoirs and Their Role in Enhancement of Photocatalytic Hydrogen Generation. *Chem. Commun.* **2016**, *52*, 9371-9374.

(14)   Kowacs, T.; O'Reilly, L.; Pan, Q.; Huijser, A.; Lang, P.; Rau, S.; Browne, W. R.; Pryce, M. T.; Vos, J. G. Subtle Changes to Peripheral Ligands Enable High Turnover Numbers for Photocatalytic Hydrogen Generation with Supramolecular Photocatalysts. *Inorg. Chem.* **2016**, *55*, 2685-2690.

(15)   Shan, B.; Schmehl, R. Photochemical Generation of Strong One-Electron Reductants via Light-Induced Electron Transfer with Reversible Donors Followed by Cross Reaction with Sacrificial Donors. *J. Phys. Chem. A* **2014**, *118*, 10400-10406.

(16)   Pellegrin, Y.; Odobel, F. Molecular Devices Featuring Sequential Photoinduced Charge Separations for the Storage of Multiple Redox Equivalents. *Coord. Chem. Rev.* **2011**, *255*, 2578-2593.

(17)   Hammarström, L. Accumulative Charge Separation for Solar Fuels Production: Coupling Light-Induced Single Electron Transfer to Multielectron Catalysis. *Acc. Chem. Res.* **2015**, *48*, 840-850.

(18)   Bonn, A. G.; Wenger, O. S. Photoinduced Charge Accumulation in Molecular Systems. *Chimia* **2015**, *69*, 17-21.

(19)   Konduri, R.; Ye, H. W.; MacDonnell, F. M.; Serroni, S.; Campagna, S.; Rajeshwar, K. Ruthenium Photocatalysts Capable of Reversibly Storing up to Four Electrons in a Single Acceptor Ligand: A Step Closer to Artificial Photosynthesis. *Angew. Chem. Int. Ed.* **2002**, *41*, 3185-3187.

(20)   Konduri, R.; de Tacconi, N. R.; Rajeshwar, K.; MacDonnell, F. M. Multielectron Photoreduction of a Bridged Ruthenium Dimer, $[(phen)_2Ru(tatpp)Ru(phen)_2][PF_6]_4$: Aqueous Reactivity and Chemical and Spectroelectrochemical Identification of the Photoproducts. *J. Am. Chem. Soc.* **2004**, *126*, 11621-11629.

(21)   Wouters, K. L.; de Tacconi, N. R.; Konduri, R.; Lezna, R. O.; MacDonnell, F. M. Driving Multi-Electron Reactions with Photons: Dinuclear Ruthenium Complexes Capable of Stepwise and Concerted Multi-Electron Reduction. *Photosynth. Res.* **2006**, *87*, 41-55.

(22)   Rangan, K.; Arachchige, S. M.; Brown, J. R.; Brewer, K. J. Solar Energy Conversion Using Photochemical Molecular Devices: Photocatalytic Hydrogen Production from Water Using Mixed-Metal Supramolecular Complexes. *Energy Environ. Sci.* **2009**, *2*, 410-419.

(23)   Molnar, S. M.; Nallas, G.; Bridgewater, J. S.; Brewer, K. J. Photoinitiated Electron Collection in a Mixed-Metal Trimetallic Complex of the Form $\{[(bpy)_2Ru(dpb)_2Ir]_2IrCl_2\}$ (bpy = 2,2'-Bipyridine and dpb = 2,3-Bis(2-pyridyl)benzoquinoxaline). *J. Am. Chem. Soc.* **1994**, *116*, 5206-5210.

(24)   Matt, B.; Fize, J.; Moussa, J.; Amouri, H.; Pereira, A.; Artero, V.; Izzet, G.; Proust, A. Charge Photo-Accumulation and Photocatalytic Hydrogen Evolution under Visible Light at an Iridium(III)-Photosensitized Polyoxotungstate. *Energy Environ. Sci.* **2013**, *6*, 1504-1508.

(25)   Polyansky, D.; Cabelli, D.; Muckerman, J. T.; Fujita, E.; Koizumi, T.; Fukushima, T.; Wada, T.; Tanaka, K. Photochemical and Radiolytic Production of an Organic Hydride Donor with a Ru(II) Complex Containing an NAD^+ Model Ligand. *Angew. Chem. Int. Ed.* **2007**, *46*, 4169-4172.

(26)   Bonn, A. G.; Wenger, O. S. Photoinduced Charge Accumulation by Metal Ion-Coupled Electron Transfer. *Phys. Chem. Chem. Phys.* **2015**, *17*, 24001-24010.

(27)   Knör, G.; Vogler, A.; Roffia, S.; Paolucci, F.; Balzani, V. Switchable Photoreduction Pathways of Antimony(V) Tetraphenylporphyrin. A Potential Multielectron Transfer Photosensitizer. *Chem. Commun.* **1996**, 1643-1644.

(28)   Elliott, K. J.; Harriman, A.; Le Pleux, L.; Pellegrin, Y.; Blart, E.; Mayer, C. R.; Odobel, F. A Porphyrin-Polyoxometallate Bio-Inspired Mimic for Artificial Photosynthesis. *Phys. Chem. Chem. Phys.* **2009**, *11*, 8767-8773.

(29)   Kitamoto, K.; Ogawa, M.; Ajayakumar, G.; Masaoka, S.; Kraatz, H. B.; Sakai, K. Molecular Photo-Charge-Separators Enabling Single-Pigment-Driven Multi-Electron Transfer and Storage Leading to H_2 Evolution Drom Water. *Inorg. Chem. Front.* **2016**, *3*, 671-680.

(30)   Karlsson, S.; Boixel, J.; Pellegrin, Y.; Blart, E.; Becker, H. C.; Odobel, F.; Hammarström, L. Accumulative Electron Transfer: Multiple Charge Separation in Artificial Photosynthesis. *Faraday Discuss.* **2012**, *155*, 233-252.

(31)   Karlsson, S.; Boixel, J.; Pellegrin, Y.; Blart, E.; Becker, H. C.; Odobel, F.; Hammarström, L. Accumulative Charge Separation Inspired by Photosynthesis. *J. Am. Chem. Soc.* **2010**, *132*, 17977-17979.

(32)   O'Neil, M. P.; Niemczyk, M. P.; Svec, W. A.; Gosztola, D.; Gaines, G. L.; Wasielewski, M. R. Picosecond Optical Switching Based on Biphotonic Excitation of an Electron Donor-Acceptor-Donor Molecule. *Science* **1992**, *257*, 63-65.

(33)   Imahori, H.; Hasegawa, M.; Taniguchi, S.; Aoki, M.; Okada, T.; Sakata, Y. Synthesis and Photophysical Properties of Porphyrin-Tetracyanoanthraquinodimethane-Porphyrin Triad: Photon-Dependent Molecular Switching. *Chem. Lett.* **1998**, 721-722.

(34)   Ghaddar, T. H.; Wishart, J. F.; Thompson, D. W.; Whitesell, J. K.; Fox, M. A. A Dendrimer-Based Electron Antenna: Paired Electron-Transfer Reactions in Dendrimers With a

4,4 '-Bipyridine Core and Naphthalene Peripheral Groups. *J. Am. Chem. Soc.* **2002**, *124*, 8285-8289.

(35)   Orazietti, M.; Kuss-Petermann, M.; Hamm, P.; Wenger, O. S. Light-Driven Electron Accumulation in a Molecular Pentad. *Angew. Chem. Int. Ed.* **2016**, *55*, 9407-9410.

(36)   Gosztola, D.; Niemczyk, M. P.; Svec, W.; Lukas, A. S.; Wasielewski, M. R. Excited Doublet States of Electrochemically Generated Aromatic Imide and Diimide Radical Anions. *J. Phys. Chem. A* **2000**, *104*, 6545-6551.

(37)   Büldt, L. A.; Prescimone, A.; Neuburger, M.; Wenger, O. S. Photoredox Properties of Homoleptic d^6 Metal Complexes With the Electron-Rich 4,4 ',5,5 '-Tetramethoxy-2,2 '-Bipyridine Ligand. *Eur. J. Inorg. Chem.* **2015**, 4666-4677.

(38)   Lever, A. B. P. Electrochemical Parametrization of Metal-Complex Redox Potentials, Using the Ruthenium(III) / Ruthenium(II) Couple to Generate a Ligand Electrochemical Series. *Inorg. Chem.* **1990**, *29*, 1271-1285.

(39)   Kuss-Petermann, M.; Wenger, O. S. Electron Transfer Rate Maxima at Large Donor-Acceptor Distances. *J. Am. Chem. Soc.* **2016**, *138*, 1349-1358.

(40)   Bonn, A. G.; Neuburger, M.; Wenger, O. S. Photoinduced Electron Transfer in Rhenium(I)-Oligotriarylamine Molecules. *Inorg. Chem.* **2014**, *53*, 11075-11085.

(41)   Bonn, A. G.; Yushchenko, O.; Vauthey, E.; Wenger, O. S. Photoinduced Electron Transfer in an Anthraquinone- $Ru(bpy)_3^{2+}$-Oligotriarylamine-$Ru(bpy)_3^{2+}$-Anthraquinone Pentad. *Inorg. Chem.* **2016**, *55*, 2894-2899.

(42)   Hoffman, M. Z.; Bolletta, F.; Moggi, L.; Hug, G. L. Rate Constants for the Quenching of Excited-States of Metal-Complexes in Fluid Solution. *J. Phys. Chem. Ref. Data* **1989**, *18*, 219-544.

(43)   Suzuki, M.; Waraksa, C. C.; Mallouk, T. E.; Nakayama, H.; Hanabusa, K. Enhanced Photocatalytic Reduction of Methyl Viologen by Self-Assembling Ruthenium(II)poly(pyridyl) Complexes with L-Lysine Containing Side Chains. *J. Phys. Chem. B* **2002**, *106*, 4227-4231.

(44)   Delaive, P. J.; Foreman, T. K.; Giannotti, C.; Whitten, D. G. Photoinduced Electron-Transfer Reactions of Transition-Metal Complexes with Amines - Mechanistic Studies of Alternate Pathways to Back Electron-Transfer. *J. Am. Chem. Soc.* **1980**, *102*, 5627-5631.

(45)   Summers, P. A.; Dawson, J.; Ghiotto, F.; Hanson-Heine, M. W. D.; Vuong, K. Q.; Davies, E. S.; Sun, X. Z.; Besley, N. A.; McMaster, J.; George, M. W.; Schröder, M. Photochemical Dihydrogen Production Using an Analogue of the Active Site of NiFe Hydrogenase. *Inorg. Chem.* **2014**, *53*, 4430-4439.

(46)   Cohen, S. G.; Parola, A.; Parsons, G. H. Photoreduction by Amines. *Chem. Rev.* **1973**, *73*, 141-161.

(47)   Probst, B.; Rodenberg, A.; Guttentag, M.; Hamm, P.; Alberto, R. A Highly Stable Rhenium-Cobalt System for Photocatalytic H_2 Production: Unraveling the Performance-Limiting Steps. *Inorg. Chem.* **2010**, *49*, 6453-6460.

(48)   Zhu, X. Q.; Mu, Y. Y.; Li, X. T. What Are the Differences between Ascorbic Acid and NADH as Hydride and Electron Sources in Vivo on Thermodynamics, Kinetics, and Mechanism? *J. Phys. Chem. B* **2011**, *115*, 14794-14811.

(49)   Neshvad, G.; Hoffman, M. Z. Reductive Quenching of the Luminescent Excited-State of Tris(2,2'-Bipyrazine)ruthenium(2+) Ion in Aqueous Solution. *J. Phys. Chem.* **1989**, *93*, 2445-2452.

(50)   Lambert, C.; Nöll, G. The Class II/III Transition in Triarylamine Redox Systems. *J. Am. Chem. Soc.* **1999**, *121*, 8434-8442.

(51)   Sreenath, K.; Thomas, T. G.; Gopidas, K. R. Cu(II) Mediated Generation and Spectroscopic Study of the Tris(4-anisyl)amine Radical Cation and Dication. Unusually Shielded Chemical Shifts in the Dication. *Org. Lett.* **2011**, *13*, 1134-1137.

(52)   Hankache, J.; Wenger, O. S. Microsecond Charge Recombination in a Linear Triarylamine-Ru(bpy)$_3{}^{2+}$-Anthraquinone Triad. *Chem. Commun.* **2011**, *47*, 10145-10147.

(53)   Fukuzumi, S.; Ohkubo, K.; Morimoto, Y. Mechanisms of Metal Ion-Coupled Electron Transfer. *Phys. Chem. Chem. Phys.* **2012**, *14*, 8472-8484.

(54)   Okamoto, K.; Mori, Y.; Yamada, H.; Imahori, H.; Fukuzumi, S. Effects of Metal Ions on Photoinduced Electron Transfer in Zinc Porphyrin-Naphthalenediimide Linked Systems. *Chem. Eur. J.* **2004**, *10*, 474-483.

(55)   Guo, D.; Knight, T. E.; McCusker, J. K. Angular Momentum Conservation in Dipolar Energy Transfer. *Science* **2011**, *334*, 1684-1687.

(56)   Kuss-Petermann, M.; Wenger, O. S. Pump-Pump-Probe Spectroscopy of a Molecular Triad Monitoring Detrimental Processes for Photoinduced Charge Accumulation. *Helv. Chim. Acta* **2016**, doi: 10.1002/hlca.201600283.

(57)   Mayer, J. M. Proton-Coupled Electron Transfer: A Reaction Chemist's View. *Annu. Rev. Phys. Chem.* **2004**, *55*, 363-390.

(58)   Hankache, J.; Wenger, O. S. Large Increase of the Lifetime of a Charge-Separated State in a Molecular Triad Induced by Hydrogen-Bonding Solvent. *Chem. Eur. J.* **2012**, *18*, 6443-6447.

(59)   Hankache, J.; Niemi, M.; Lemmetyinen, H.; Wenger, O. S. Hydrogen-Bonding Effects on the Formation and Lifetimes of Charge-Separated States in Molecular Triads. *J. Phys. Chem. A* **2012**, *116*, 8159-8168.

(60)   Quan, M.; Sanchez, D.; Wasylkiw, M. F.; Smith, D. K. Voltammetry of Quinones in Unbuffered Aqueous Solution: Reassessing the Roles of Proton Transfer and Hydrogen Bonding in the Aqueous Electrochemistry of Quinones. *J. Am. Chem. Soc.* **2007**, *129*, 12847-12856.

(61)   Warren, J. J.; Tronic, T. A.; Mayer, J. M. Thermochemistry of Proton-Coupled Electron Transfer Reagents and its Implications. *Chem. Rev.* **2010**, *110*, 6961-7001.

(62)   Markle, T. F.; Mayer, J. M. Concerted Proton-Electron Transfer in Pyridylphenols: The Importance of the Hydrogen Bond. *Angew. Chem. Int. Ed.* **2008**, *47*, 738-740.

(63)   Rhile, I. J.; Markle, T. F.; Nagao, H.; DiPasquale, A. G.; Lam, O. P.; Lockwood, M. A.; Rotter, K.; Mayer, J. M. Concerted Proton-Electron Transfer in the Oxidation of Hydrogen-Bonded Phenols. *J. Am. Chem. Soc.* **2006**, *128*, 6075-6088.

(64)   Costentin, C.; Robert, M.; Savéant, J.-M. Concerted Proton-Electron Transfers: Electrochemical and Related Approaches. *Acc. Chem. Res.* **2010**, *43*, 1019-1029.

(65)   Bronner, C.; Wenger, O. S. Kinetic Isotope Effects in Reductive Excited-State Quenching of $Ru(2,2\text{'-bipyrazine})_3^{2+}$ by Phenols. *J. Phys. Chem. Lett.* **2012**, *3*, 70-74.

(66)   Nomrowski, J.; Wenger, O. S. Photoinduced PCET in Ruthenium-Phenol Systems: Thermodynamic Equivalence of Uni- and Bidirectional Reactions. *Inorg. Chem.* **2015**, *54*, 3680-3687.

(67)   Moore, G. F.; Hambourger, M.; Gervaldo, M.; Poluektov, O. G.; Rajh, T.; Gust, D.; Moore, T. A.; Moore, A. L. A Bioinspired Construct that Mimics the Proton Coupled Electron Transfer between $P680^{\bullet+}$ and the Tyr_z-His_{190} Pair of Photosystem II. *J. Am. Chem. Soc.* **2008**, *130*, 10466-10467.

(68)   Chen, J.; Kuss-Petermann, M.; Wenger, O. S. Distance Dependence of Bidirectional Concerted Proton-Electron Transfer in Phenol-$Ru(2,2\text{'-bipyridine})_3^{2+}$ Dyads. *Chem. Eur. J.* **2014**, *20*, 4098-4104.

(69)   Lachaud, T.; Quaranta, A.; Pellegrin, Y.; Dorlet, P.; Charlot, M. F.; Un, S.; Leibl, W.; Aukauloo, A. A Biomimetic Model of the Electron Transfer between P-680 and the Tyr_z-His_{190} Pair of PSII. *Angew. Chem. Int. Ed.* **2005**, *44*, 1536-1540.

(70)   Wenger, O. S. Proton-Coupled Electron Transfer with Photoexcited Metal Complexes. *Acc. Chem. Res.* **2013**, *46*, 1517-1526.

(71)   Wenger, O. S. Proton-Coupled Electron Transfer with Photoexcited Ruthenium(II), Rhenium(I), and Iridium(III) Complexes. *Coord. Chem. Rev.* **2015**, *282*, 150-158.

(72)   Eisenhart, T. T.; Dempsey, J. L. Photo-induced Proton-Coupled Electron Transfer Reactions of Acridine Orange: Comprehensive Spectral and Kinetics Analysis. *J. Am. Chem. Soc.* **2014**, *136*, 12221-12224.

(73)   Concepcion, J. J.; Brennaman, M. K.; Deyton, J. R.; Lebedeva, N. V.; Forbes, M. D. E.; Papanikolas, J. M.; Meyer, T. J. Excited-State Quenching by Proton-Coupled Electron Transfer. *J. Am. Chem. Soc.* **2007**, *129*, 6968-6969.

(74)   Bronner, C.; Wenger, O. S. Long-Range Proton-Coupled Electron Transfer in Phenol-Ru(2,2 '-Bipyrazine)$_3^{2+}$ Dyads. *Phys. Chem. Chem. Phys.* **2014**, *16*, 3617-3622.

(75)   Sproviero, E. M.; Gascon, J. A.; McEvoy, J. P.; Brudvig, G. W.; Batista, V. S. Quantum Mechanics/Molecular Mechanics Study of the Catalytic Cycle of Water Splitting in Photosystem II. *J. Am. Chem. Soc.* **2008**, *130*, 3428-3442.

(76)   Sartorel, A.; Bonchio, M.; Campagna, S.; Scandola, F. Tetrametallic Molecular Catalysts for Photochemical Water Oxidation. *Chem. Soc. Rev.* **2013**, *42*, 2262-2280.

Table of Contents Graphic and Synopsis
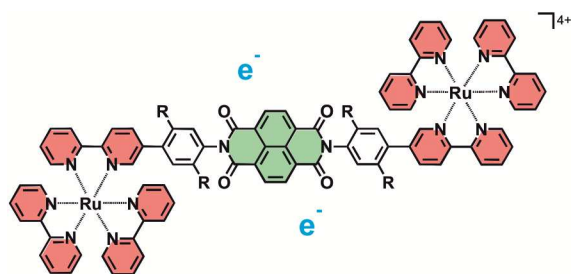
A series of intra- and intermolecular photoinduced electron transfer processes leads to accumulation of two electrons on a naphthalene diimide unit in a molecular triad, using sacrificial reagents as electron donors. In a molecular pentad with covalently attached reversible donors, electron accumulation remained unobserved.